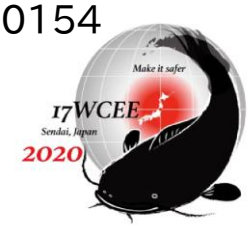

17th World Conference on Earthquake Engineering, 17WCEE

Sendai, Japan- September13th to 18th 2020

EXPERIMENTAL VS NUMERICAL CORRELATION FOR A SHAKING TABLE TEST OF A CONCRETE PRECAST MODEL STRUCTURE EQUIPPED WITH SLB DEVICES

M. Pantoja [1], H. Gonzales [2], L.M. Bozzo [3], G.Bozzo[4], J. Ramirez[5]

[1]*Structural engineer, PostensaSAC Lima (Peru), info.postensa@gmail.com*
[2]*Msc., PhD., Structural engineer, Postensa SAC Lima-Peru, ing@postensa.pe*
[3]*Msc., PhD., General Director, Luis Bozzo Estructuras y Proyectos S.L. Barcelona (Spain) , info@luisbozzo.com*
[4]*Msc. Structural engineer (in process), Universitat Politècnica de Catalunya Barcelona (Spain), guillebozzo96@gmail.com*
[5]*Msc. Structural engineer (in process), Universitat Politècnica de Catalunya, Barcelona (Spain), junior.rm,.31.10@gmail.com*

Abstract

This work presents the experimental and numerical correlation for ~~a~~ two degrees of freedom precast concrete structure equipped with SLB devices. The model was tested at the PUCP unidirectional shaking table in Peru. The shaking table limitations conditioned the whole module. The effectiveness of SLB dissipators increases as the bare structure is more flexible. However, the maximum weight on the shaking table is 150kN and the maximum height of the model 6m with 4.4 m width. The flexible structure is achieved by 5.3m height 22cm × 22cm section columns and a concentrated mass on top. Stiffness and ductility of the structure is achieved by uncoupled 10cm thick walls on both sides equipped with a single SLB device at the top middle section. If these two uncoupled walls had been installed from the shaking table base, the overall 150kN weight condition would have been exceeded. Therefore, the walls were placed 170cm from the base in order to verify the weight condition; however, that leads to a strong discontinuity. This discontinuity is not a problem for structures equipped with SLBs, since the maximum force transferred by the devices is limited and verified before manufacturing. A particular advantage of the SLB devices is that they are manufactured after material testing of the base steel plate so their final dimensions are adjusted. The paper describes the unidirectional tensile test in order to obtain the complete stress – strain curve for the steel plate. The "engineering curve" is converted into a "real stress – strain curved" for a FEM of the SLB device. According to nonlinear geometric and material properties and using ANSYS program the simplified hysteretic devices properties are generated for the specific material used for their manufacturing.

The model set up on the shaking table consists of LVDTs as well as accelerometers on top and on the uncoupled walls. The test schedule consists of twelve phases. The first four were characterization of the structural period under free vibration and sinusoidal frequency sweep tests for the model with and without SLB devices. The subsequent 3 phases were for the 1974 Lima earthquake increasing its peak acceleration up to 0.927g. Similarly, the subsequent 3 phases were for the 1970 Lima earthquake increasing its peak acceleration up to 1.367g. Finally, the remaining two phases were done after uninstalling the devices. An important observation is that in all the tests, the devices were the same and their yielding, due to its initially high stiffness, started from phase 1.

The experimental results are compared to numerical values using simple Wen's hysteretic model and nonlinear time history analysis. The peak acceleration for phase 6 showed a 5% difference. For the same phase the top displacement difference is only 2%. The peak acceleration and displacement for phases 4 and 5 varies more than phase 6. In all cases, as the signal increases, its base acceleration the correlation is improved, most probably due to the fact that for smaller vibrations there are various uncertainties at the hinged connections such as friction coefficient and minimum rotation stiffness.

Key words: SLB devices; experimental numerical correlation; experimental model; dissipators; prefabrication.

1. Introduction

In Peru and other countries, there is a significant housing deficit which is difficult to mitigate using conventional construction techniques. Precast and industrial construction can be an effective way to mitigate this problem in particular for medium-sized house buildings. The actual widespread solution for low-income families in Peru is based on the so-called “low ductility wall system”. In this solution, thin walls are cast on site in both directions at spans no larger than, typically, 3m to 4m. The walls have just one centered mesh and their thickness is maximum 10cm. A special false framework allows for fast construction although it cannot be as fast as an industrialized precast one. Moreover, the 3m to 4m spans provide a poor architectonical and quality solution for users and the 100mm thick walls do not allow any present or future change (such as it is usually the case for electrical or even sanitary installations). Finally, a large amount of concrete is required and the final structure, as its name indicates, has low ductility. As a consequence, a Peruvian Housing Minister (MVCS) project proposing a precast concrete structure solution incorporating energy dissipators was requested and this article presents parts of its results and conclusions.

A significant part of the MVCS project was to perform an experimental test and its numerical correlation. The precast solution incorporates continuous columns and hinged beams in order to have a very flexible bare system [1] which, when combined with stiff energy dissipation devices (such as SLB), provides an optimal seismic response. Furthermore, the hinged beams solution allows for a very fast construction time avoiding complex on-site labor such as provide continuity in the beams. Fig. 1 shows an elevation view of the precast structure equipped with the devices on the shaking table. The whole module was built in a neighborhood on the outskirts of Lima and transported using simple cranes to the Catholic University Structures Laboratory. Due to very strict shaking table limitations, the model has special characteristics which are commented in section 2.1.

(a) (b)

Fig. 1 – (a) Elevation view of the model equipped with energy dissipators SLB on the shaking table

(b)Pinned end connections for the beams using high-quality carbon steel

The main objective of the shaking table tests was to calibrate simple numerical analysis models to predict the experimental results. This implies that rather than validating the specific model on the shaking table, the findings of the project would be useful for a wide range of applications. For instance, conclusions or modeling recommendations can be also applied for public and private buildings that require structural retrofit to withstand earthquakes.

2. Brief description of the SLB system and its numerical analysis for the devices

2.1Description of the model

Even though the Catholic University shaking table is the largest in Peru, it has strong limitations conditioning the module. Specifically, the height cannot be taller than 6m, the width 4.4m and more

important the total weight cannot overpass 15Ton. Furthermore, for an optimal combination of precast and stiff dissipators, the bare or precast structure should be as flexible as possible [1]. As a consequence, the model structure has a height of 5.8m and a base dimension of 3.0 m parallel to the direction of movement and the resulting total weight was approximately 140kN. The walls that support the SLB devices make a significant contribution to the total weight and therefore they are not prolonged to the basement (see Fig. 1). It should be taken into account that for a conventional solution this strong discontinuity would generate an over strength local problem which is not the case using SLB devices. As previously stated, the final dimensions for these devices are adjusted according to the tensile test for their base steel plates.

In total, two SLB energy dissipators were installed on top of the uncoupled reinforced concrete walls. Fig. 2(a) shows the dimensions seen from above of the module tested and the location of the walls parallel to the direction of movement. Figure 2(b) shows the connection details of the SLB on the uncoupled walls with the top beam of the module structure. Table 1 shows the characteristics of all the structural elements of the tested module.

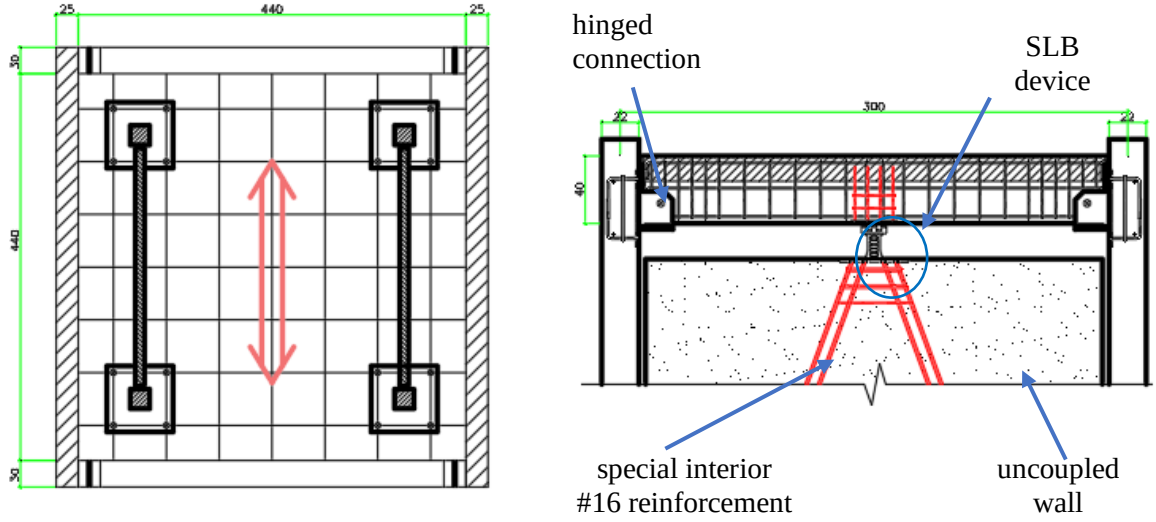

(a) (b)

Fig. 2 – Module: (a) view from above and (b) details of the connection of the SLB

Table 1 – Characteristics of all the structural elements tested

Structural elements	Number	Dimensions (mm)	Compressive strength f'c (MPa)	Yield strength (MPa)
Footings	4	750×750×600	28	-
Columns	4	220×220×5300	28	-
Beams	2	220×400×2730	28	-
Uncoupled walls	2	2700×2700×100	35	-
Precast slabs	3	925×3000×150	28	-
Bar reinforcing	-	-	-	420
Welded-wire mesh	-	-	-	500
Tubular steel beams to support decoupled walls	2	[]200×200×6	-	253
Tubular steel braces	4	[]100×100×5	-	253
Roof-level tubular steel	2	[]150×150×6	-	253
SLB energy dissipators	2	75×150×16	-	253

For the construction of all prefabricated structural elements, the mixture of concrete was considered with a maximum aggregate size of 1/4 inch. (6.35 mm), high range water reducing admixture and super plasticizer without delay. Quality control tests using concrete cylinders indicated that the average compressive strengths were higher than the design ones. The reinforcement steel used in the concrete elements consisted of corrugated bars, ASTM 615 grade 60 steel (Fy = 420MPa). For the uncoupled walls 10 cm thick and with the purpose of reducing the construction time, welded-wire meshes were used (Fy = 500MPa) distributed in two layers.

Prefabricated elements such as concrete beams and metal tubular diagonals were connected to the columns by hinges, although some bending moments are transferred due to friction at their supports. Likewise, in order to soften the impact between beams and columns that might exist, neoprene plates were placed on steel brackets embedded in the columns to support the beams (see Fig.1b).To ensure that the connection is fully hinged, it was proposed to place a high-quality carbon steel pin (AISI H-1045) with the yield strength of approximately fy = 350MPa. This element crosses the concrete beam transversely and the stiffener of the bracket, as shown in Fig.1b [2].

2.2 Seismic signals for the test

The seismic records considered for the shaking table test correspond to two earthquakes that occurred on the Peruvian coast, which produced considerable damage to the structures at that time: (1) Earthquake of May 31, 1970 component EW (1970 Lima Earthquake) and (2) Earthquake of the January 5, 1974 (1974 Lima Earthquake). For both earthquakes, the EW component was considered.

These two earthquakes were significantly scaled because the strong record database on the Peruvian cost is still very limited and the main objective was to maintain the local frequency content. The type of soil where these signals were registered corresponds to a firm ground so they generate a resonant period of short range. Again, this resonant period had to be short because the shaking table has a limitation of 0.15m of movement, so it is limited to seismic records on rigid or medium ground. Figure 3 shows the response spectrum of May 31, 1970; and January 5th, 1974 Earthquakes. Table 2 shows the maximum accelerations recorded for each component of the seismic signals considered. Figure 3shows the response spectrum of May 31, 1970; and January 5th, 1974 Earthquakes. Table 2 shows the maximum accelerations recorded for each component of the seismic signals considered.

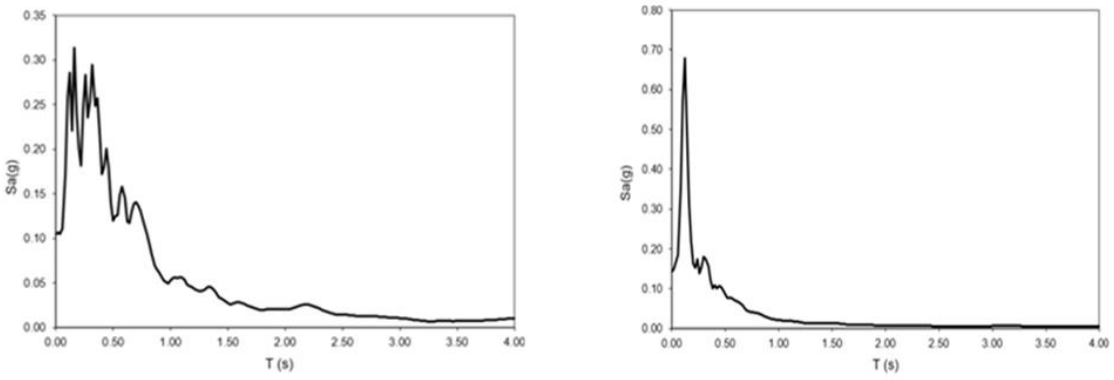

(a) (b)

Fig. 3 – Response spectrums of (a) Earthquake of May 31, 1970 and (b) Earthquake of January 5th, 1974 [2].

The test consisted of applying real earthquakes scaled at different levels of peak accelerations. Before the application of the seismic signals, a frequency sweep was made in order to know the fundamental period of the structure with and without SLB dissipators.

This method consists of applying a frequency range to the structure until it goes into resonance so that we could determine fundamental periods of the structure. For this, five sinusoidal cycles were applied to determine amplification levels, but limiting their magnitude and duration in order to avoid damaging the structure [3].

Table 2 – Maximum accelerations recorded for each seismic signal considered in the test

Accelerograms	Station	EW Component	NS Component
Earthquake of May 31,1970	Parque de la Reserva	0.10g	0.10g
Earthquake of January 5, 1974	Zarate	0.14g	0.16g

Figure 4 shows the frequency sweep applied. For the structure with SLB dissipators, the frequency range was 4 to 6 Hz, and for the structure without dissipators it was 1 to 2 Hz. In this way, the fundamental period of 0.171s (5.847Hz) and 0.529s (1.89Hz) were obtained for each structure (with and without dissipators). It should be taken into account that the fundamental structural period would vary, according to the devices yielding from 0.171s to 0.529s. This means that the structural period will instantly range in the actual resonance period of the signals (see Fig. 3). This implies the tests are a strong condition for the precast model. Furthermore, it would have been desirable for the actual "bare frame period" to be much longer (for example 2 or 3s) but again the shaking table limitations prevented this.

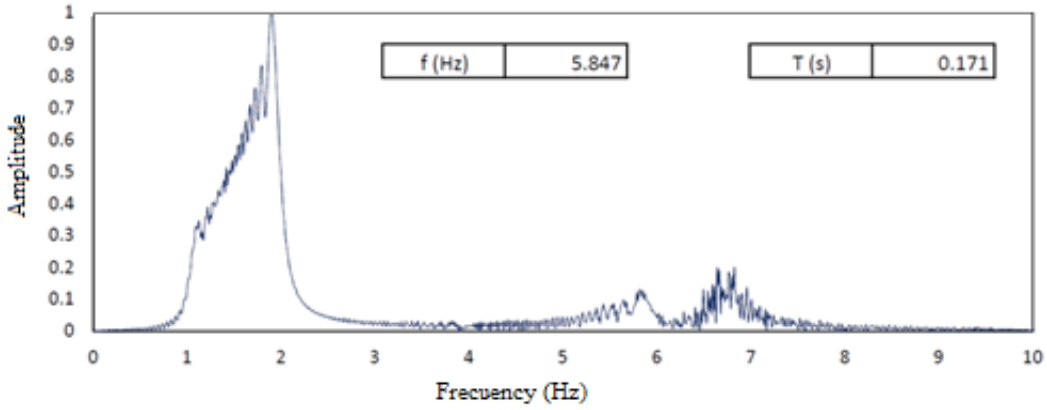

Fig. 4 – Frequency sweep test for the structure with and without dissipators (f2 = 5.85Hz and f1 = 1.89Hz)

The test with dissipators consists of six phases. The first three were using the Lima 1974 earthquake while the other three were using the 1970 one. Table 3 shows the escalated accelerations in the first three phases for the EW component of the 1974 Lima earthquake and the last three correspond to the EW component of the Lima earthquake of 1970.

Table 3 – Scaled accelerations for the 1974 Lima and 1970 Lima earthquakes

Phase	Phase 1	Phase 2	Phase 3	Phase 4	Phase 5	Phase 6
Scaled acceleration to	0.181g	0.653g	0.927g	0.44g	0.88g	1.367g

The numerical-experimental correlation was carried out for the last three strongest phases, which are phases 4, 5 and 6. This is because, in the previous phases various factors affected the numerical calibration, such as the internal friction in the articulated connections of the ends of the prefabricated elements. A future more precise model including all phases would require incorporating a frictional rotational spring at the beam hinges.

3. Global numerical model and parametric study

3.1 Numerical Model

A simple model using ETABS program was developed to simulate experimental results for the last 3 phases of the test. The structural model corresponds to beams, columns axes and the uncoupled walls supported in the middle of the steel beams. Experimental accelerations were measured at the shaking table and applied to the model.

A first aspect to consider was deciding the definition of footings in the structural model. For this reason, three different structural models were performed and are described below (see Fig. 5):

- Model 1: Structure without fixed footings at the base of the four columns (model height is 5.2m).

- Model 2: Structure with modified cross sections of columns and the same dimensions as test footings (model height is 5.8m).

- Model 3: Same structure as second model, but reducing the height of the footing from 60cm to 30cm (that is, at its axis and with a model height of 5.5m).

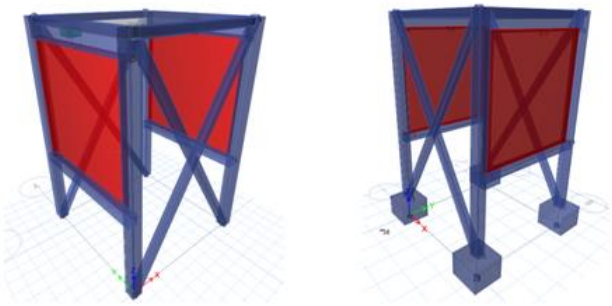

Fig. 5 – Structural models 1, 2 and 3 in ETABS program

From the results obtained, the effect of considering the foundation was not significant, but for greater precision, the footing (model 2) was considered. Using the Rayleigh model, global structural damping was assumed at 2% for the period of vibration corresponding to the structure with dissipators in yielding (T = 0.529s) and 5% for the initial period (T = 0.171s). The Rayleigh model is suitable for calculating damping since there is strong non-linear behavior in a structure subject to dynamic loads.

The beams on which the wall rests are articulated at their ends. They are simulated as tubular steel frame elements. The upper beams, parallel to the Y-axis, which is where the loads act, are made of reinforced concrete and, as indicated, are pinned-end. The other two upper beams are tubular steel and have been modeled also as articulated frame elements.

The columns are modeled as frame elements with plastic hinges at the base, although, they were not activated. The plastic hinges were defined accordingly to FEMA 356 regulations [4].

3.2 SLB Energy dissipators

The theory of plasticity [5] and finite element techniques [6] allows the precise study of the non-linear response of energy dissipation devices. A general element can be modeled using, for example, 3D solid elements of 2D shell ones using programs such as ANSYS [7]. This model would allow detection of local concentration of stresses and verifying plasticity areas and demands. However, for practical analysis, the results would be too complex and, consequently, it is convenient to condense them in special elements such as simple hysteretic models.

In this research to numerically characterize the behavior of SLB dissipators, the Wen model is used in order to consider only four parameters: K_1, fy, K_2 / K_1 and the coefficient "n". However, in section 4 it is decided to fix this coefficient to 2 so there are only 3 parameters that define the hysteretic properties for these devices. Even though the model is almost 6m high, the required yielding force at the devices resulted too small and they were not at the standard design tables [8]. Consequently, a special device was manufactured only for the tested module with an 18kN initial yielding force objective. The design process consists in obtaining the tensile strain–stress curve for the steel plate selected for the manufactured device. The curve was correlated to the engineering relation using the following expressions:

$$\sigma_R = \frac{\sigma}{1-1.5\varepsilon} \quad (1)$$

$$\varepsilon_R = \ln(1+\varepsilon) \quad (2)$$

Where $\varepsilon_R$is true strain, σ_R is true stress, ε is engineering strain and σ is engineering stress.

Given the battlement connection, the model was fixed at the base and free at the other and without axial force (see Fig. 6a). With this procedure the monotonic curve of the dissipator was obtained until a certain maximum objective displacement, which for these devices is fixed at 20mm. By drawing the initial tangent, the second slope is obtained equating the areas above and below the two lines and the monotonic curve. Then it is simple to obtain the coefficients K_1 and K_2 as well as the yielding force (fy) of the dissipator by the intersection of the two lines. With the objective to install any device into the battlement connection, a tolerance is required. Therefore, the end point of the straight line of K_1 is displaced 0.5mm and the new values for K_1, K_2 and fy are obtained. Figure 6b shows the three curves discussed above.

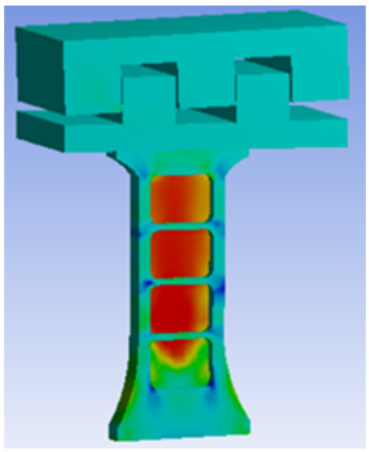

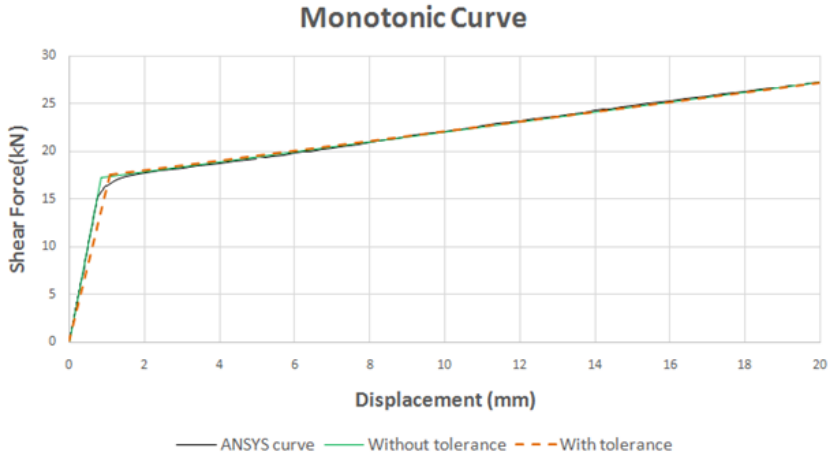

(a) (b)

Fig. 6 – (a) FEM of SLB dissipator in ANSYS (b) Monotonic curves of SLB

As a result, the following four parameters were obtained to represent the devices using the Wen´s model [9]: Elastic stiffness: K_1 = 16000 kN.m; Yield strength: Fy = 17.56 kN; Relationship between elastic and post-yield stiffness: K_2 / K_1 = 0.031875 and Yielding exponent: n = 2.

Table 4 presents device modeling parameters considering or not the aforementioned 0,5mm tolerance at the battlement connection. As can be observed, the initial stiffness and the yielding displacement in particularly change about 20% to 25%. However, the difference is considered relatively small for practical purposes because the resulting value is still big and the yielding displacement still small.

Table 4–Summary of results for monotonic curves

Design parameters for energy dissipators Shear Link Bozzo (SLB)							
SLB dissipators	**Dissipator thickness (mm)**	**Thickness of dissipative windows (mm)**	**Initial stiffness K_1 (kN/m)**	**Yield-post stiffness K_2 (kN/mm)**	**Yield displacement DY (mm)**	**Tensile force Fy (kN)**	**Max tensile force (kN)**
SLB (without tolerance)	19	2	20.00	0.52	0.86	17.24	82.02
SLB (Tolerance of 0.5mm)	19	2	16.00	0.51	1.10	17.56	82.02

3.3 Modulus of elasticity of concrete

Theoretical properties of the modulus of elasticity of concrete were obtained from design expressions of the ACI 318-14 based on the compressive strength of concrete in columns [10]. Additionally, three specimens were tested by audiometry to calibrate more accurately their values. The audiometry procedure consists in hitting the concrete cylinders with a hammer measuring the resulting noise. This record is processed and, according to the wave propagation theory an application developed by Professor Francisco de la Mora from the "Universidad Panamericana de Guadalajara" [11] the modulus instantaneous value is determined. Table 5 shows a summary of results.

Table 5– Comparison of modulus of elasticity for different compressive strength of concretes

Concrete Specimen	**13/02/2018**	**ACI-318**	**28/03/2018**	**ACI-318**	**20/03/2018**	**Ratio Audiom/Test**
	Theoretical	$E = 1510\sqrt{f'c}$	**PUCP Laboratory Test**	$E = 1510\sqrt{f'c}$	**Audiometry**	
	f'c [MPa]	**E [MPa]**	**f'c [MPa]**	**E [MPa]**	**E [MPa]**	
Column 1	28	24778.5	41.49	30162.5	35598.0	1.180
Column 2	28	24778.5	50.20	33177.8	36382.5	1.097
Column 3	28	24778.5	36.97	28472.2	33930.9	1.192
Concrete Specimen Dimensions: 4-in× 8-in					35 MPa	
Weight: 3790 gr					Concrete Strength	

4. Numerical calibration of experimental results

The fundamental period of module was numerically obtained using the concrete modulus of elasticity values obtained by audiometry instead of using the ACI provisions. The experimental stiff period was 0.171s and the numerical value was only 4% different, as shown in Table 6.

Table 6– Experimental and numerical fundamental periods

Model	**Fundamental period (s)**	**Error**
Experimental	0.171 s	
Numerical (Model 1)	0.178 s	4%

Once the fundamental period was calibrated, two straightforward models were developed: (1) without plastic hinges at column bases and (2) model with potential plastic hinges at the base. Since no yielding was observed at the column bases during the test, the first model was used for subsequent analysis. Table 7 shows maximum roof accelerations and base accelerations for phases 4, 5 and 6 (1970 Lima earthquake) and considering parameter "n" as 2 or 1. In general, a good correlation is observed, particularly for the parameter n=2 and for the strongest signal. The latter is explained because the rotational stiffness at the connections is

not considered in this simple model and it significantly affects the response for low intensity motions. In any case and for practical applications the difference in peak values is acceptable. Figure 8 shows similar results, but graphically it is more evident when the signal intensity increases the correlation numerical-experimental improves.

Table 7– Roof accelerations (g) vs. base accelerations(g) for the phases 4, 5 and 6 (1970 Lima earthquake)

Phase	Numerical Model		Experimental Model		Acceleration error	
	Base Acceleration (g)	Roof Acceleration (g)	Base Acceleration(g)	Roof Acceleration(g)	n=2	n=1
Phase 4	0.439	0.591	0.439	0.772	23.0%	27.5%
Phase 5	0.881	1.130	0.881	1.369	17.0%	28.6%
Phase 6	1.368	1.793	1.368	1.702	5.0%	7.6%

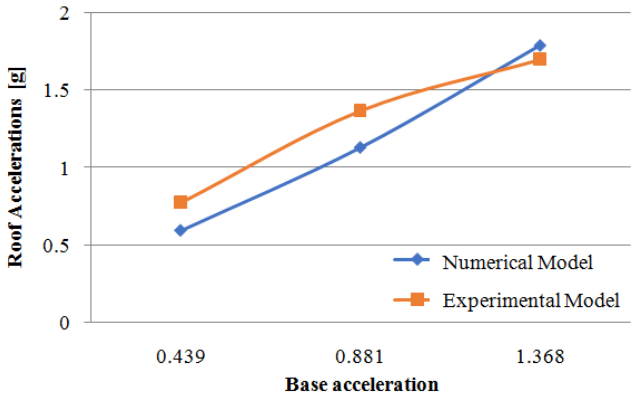

Fig. 7– Roof acceleration vs. base acceleration for experimental and numerical models

Table 8 shows the maximum roof displacements (mm) and accelerations at the base (g) for phases 4, 5 and 6 (1970 Lima earthquake) and considering parameter “n” as 2 or 1.Even though the difference between yielding exponents of "n=1" or "n = 2" is small, a value of "n" = 1 provides in this case, better results for displacements. Recently, for the strongest signal the results are clearly improved and likewise the explanation is that the rotational stiffness at the connections is not considered in this model. The friction at the hinges supports significantly affects the response for low intensity motions. In any case and for practical applications, the difference in peak values is acceptable. Figure 8 represents similar results but shows more graphically that as the signal increases, the correlation is improved. With respect to the Wen exponent, the differences are minimal and are not considered representative for a practical analysis, so the usual value of “n = 2” continues to be recommended.

Table 8– Roof displacements (mm) vs. Base accelerations (g) for phases 4, 5 and 6 (Lima 1970 earthquake)

Phase	Numerical Model		Experimental Model		Displacement error	
	Base Acceleration (g)	Roof displacements (mm)	Base Acceleration (g)	Roof displacements (mm)	n=2	n=1
Phase 4	0.439	6.465	0.439	13.578	52%	52.2%
Phase 5	0.881	16.68	0.881	27.440	39%	35.6%
Phase 6	1.368	40.368	1.368	41.338	2%	0.42%

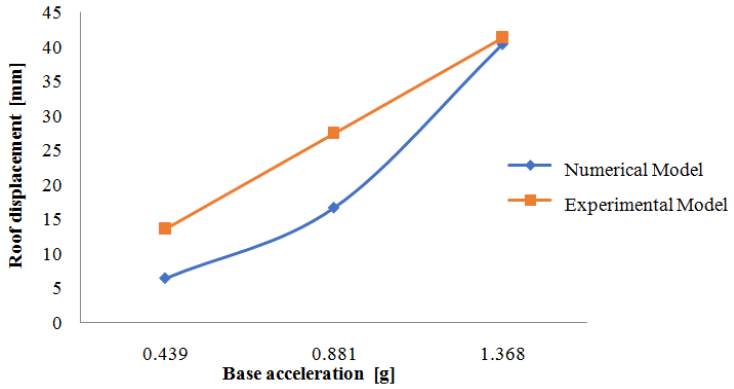

Fig. 8 – Roof displacement versus base acceleration for experimental and numerical models

Figure 9 and 10show a time history comparison between experimental and numerical accelerations and displacements, respectively, for phase 6. A great correlation is observed and the small phase mismatches that are detected can be due to the different phases being consecutive, leaving the model with slight permanent movements. That is, at the end of phase 5, for instance, the structure had a small residual displacement due to the fact that the dissipators yielded, so the global structural response was inelastic. However, for the test measurements, they always start from zero and this accumulates small numerical mismatches.

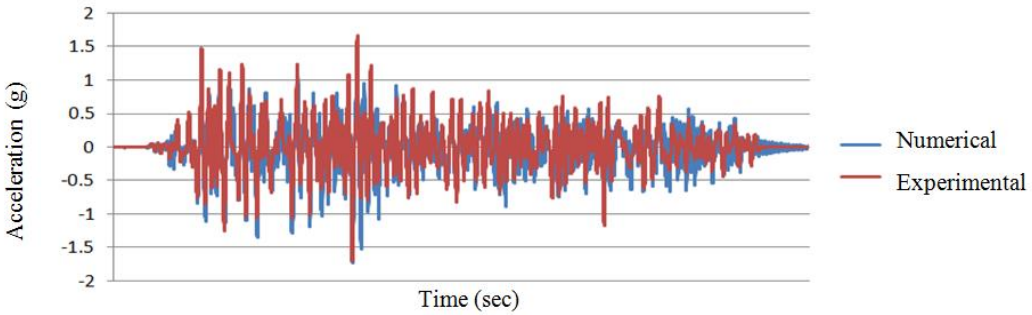

Fig. 9– Phase 6 comparisons of experimental and numerical accelerations.

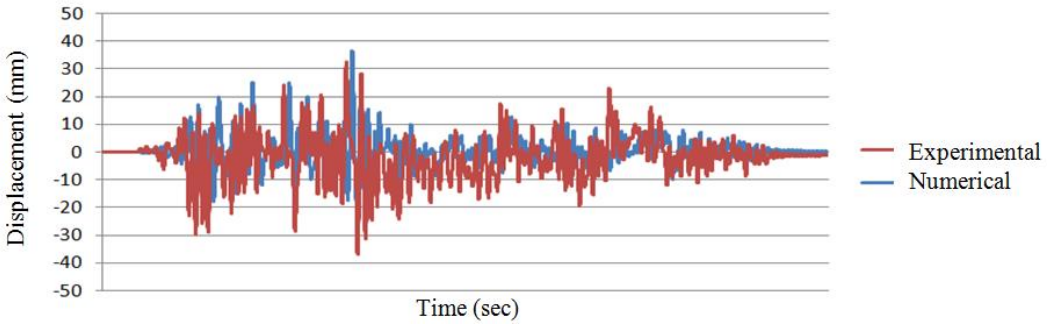

Fig. 10– Phase 6 comparisons of experimental and numerical displacements.

Finally, a comparison is presented for maximum displacements and accelerations by modifying the damping in the periods of T1 = 0.178s and Tn = 0.051s following the Rayleigh damping procedure. The previous periods correspond to the first mode and the "n" mode in which 90% modal participation is reached. In the following table, the first column represents the indicated 2% and 5% damping and the second column reducing the damping for the period T1 to 0%.

Table 9– Roof lateral displacements with 2% and 5% damping

Damping	2%_Mode 1 5%_Mode 2	0%_Mode 1 5%_Mode 2	Experimental
Roof lateral displacements Phase 6 (mm)	40.368	46.492	41.338
Error	2%	12%	

Table 10– Roof accelerations with 2% and 5% damping

Damping	2%_Mode 1 5%_Mode 2	0%_Mode 1 5%_Mode 2	Experimental
Roof acceleration Phase 6(g)	1.793	1.962	1.7016
Error	5%	15%	

A worse approximation is observed in the displacements and the accelerations assuming 0% of damping in the period T1. Therefore, the recommendation is clearly to consider in the numerical model a damping between 2% and 5% for the periods T1 and Tn (where "n" is the period in which 90% of modal participation is reached).

5. Conclusions

This work presents the results of the experimental and numerical correlation for a two-degrees-of-freedom precast concrete structure equipped with SLB devices. Dynamic nonlinear analyses have been conducted in order to simulate the seismic response of the modulus on the shaking table. Good agreement with the test results was shown even though the numerical model is quite simple. The main conclusions of this study are:

- SLB devices dissipated most of the total input seismic energy so the structural elements remained in the linear-elastic range without damage. These devices were not replaced after each test even though they yield from the first phase. This implies that they do not need to be subsequently replaced after seismic events as long as they do not exceed certain device limits.
- The hysteretic characterization of these devices can be represented by the Wen´s model. This simple model uses only four parameters to represent the response: K_1, fy, K_2 / K_1 and the coefficient "n". However, it is recommended for simplicity to fix "n" coefficient at 2 so there are only 3 parameters that define the hysteretic properties for these devices.
- In spite of the strong discontinuity generated by the uncoupled walls on the model, the columns were not overstressed and no plastic hinge was observed numerically or experimentally. This is explained by the low yielding force in the devices that control the response, restricting forces transferred to the columns.
- The proposed precast concrete structure met the continuous operational requirements in terms of providing maximum inter-storey drifts for the maximum design earthquake and without any ductility or redundancy reduction with values below 0.0035. Yielding was concentrated on the devices and the bare structure remained linear elastic
- The errors in the maximum acceleration values vary from 23% to 5% and the errors in the maximum top displacement values vary from 52% to 2%. A clear trend is that the strongest the signal the smaller the error. The values are considered acceptable to predict the behavior of the structure because the model is quite simple and there are many factors that might influence its response, such as the friction between the joints or their tolerances.

- A better or improved model would be to considerer a nonlinear frictional spring at the pinned-end beams so that represent the fact that the rotation of the beams is not free and at least a certain amount of frictional force restrains movements. This is probably the reason why the results are better calibrated for stronger motions.
- Unlike conventional constructions, this precast module with energy dissipators increases the speed of construction and reduces the time for the prompt operation of the structure. It is feasible to develop simple precast structures equipped with energy dissipators whose costs are affordable and meet current standards for earthquake-resistant design.

6. Acknowledgements

This work has received financial support from the Ministry of Housing, Construction and Sanitation of Peru. The authors are also thankful to Gustavo Salinas and Manuel Bermudez who contributed significantly to the shaking table test.

7. References

[1] L. Bozzo, Gaxiola G (2015): *El Concepto "Rigido-Flexible-Ductil" y las conexiones SLB.* XX Congreso Nacional de Ingeniería Sísmica, Acapulco, Mexico

[2] Bozzo L, Gonzales H, Salinas G, Pantoja M (2018): *Servicio de consultoría para elaborar un estudio sobre la aplicación de disipadores sísmicos en estructuras nuevas y existentes*. Lima, Peru. (in Spanish).

[3] PUCP (2018): *Ensayo dinámico de simulación sísmica de un módulo prefabricado-protegido con disipadores de fluencia, hecho de concreto armado y acero*. Lima, Peru. (in Spanish).

[4] Bozzo G (2018): *Simulación de un ensayo en mesa vibrante de una estructura con dispositivos de disipación sísmica para viviendas de bajo coste (Tesis de grado).* Universitat Politècnica de Catalunya, Barcelona, Spain (in Spanish).

[5] Chen W.F. y D.J. Han (1988). *Plasticity for Structural Engineers*. Springer-Verlag, New York.

[6] Zienkiewicz, O. C., Taylor, R. L., & Taylor, R. L. (1977). *The finite element method (Vol. 3)*, London: McGraw-hill.

[7] Lee H. H. (2015): *Finite element simulations with ANSYS workbench 16*. SDC publications.

[8] Bozzo L, et al. (2019): *Manual de procedimiento para el diseño con SLB*, Barcelona, Spain. (in Spanish).

[9] Wen Y.K., (1976): Method for Random Vibration of Hysteretic Systems," Journal of the Engineering Mechanics Division, ASCE, Vol. 102, No. EM2.

[10] American Concrete Institute (ACI) – Committee 318 (2014): *Building Code Requirements for Structural Concrete*. American Concrete Institute. Detroit.

[11] Mora F (2018): Personal communication.

